e20 Atlas of Noninvasive Cardiac Imaging

Rick Nishimura, Raymond J. Gibbons, James F. Glockner, A. Jamil Tajik

Noninvasive cardiac imaging is essential to the diagnosis and management of patients with known or suspected cardiovascular disease. Chapter 222 describes the principles and clinical applications of these important techniques. This atlas supplements Chap. 222. It provides "real time" image clips, as they are viewed in clinical practice, as well as additional static images.

VIDEO e20-1 Real-time echocardiographic images of a patient with a normal heart. ***A.*** (Play video) Parasternal long axis view. ***B.*** (Play video) Parasternal short axis view. ***C.*** (Play video) Apical four-chamber view. There is symmetric contraction of the ventricles, evidenced by a decrease in cavity size and an increase in wall thickness during systole.

Echocardiographic imaging is performed from multiple acoustic windows with different transducer rotations so that the entire heart and great vessels can be displayed in various planes. Most information from a study is obtained from a visual analysis of the two-dimensional images, although objective measurements of cardiac dimensions can be made (see **Fig. e20-1**).

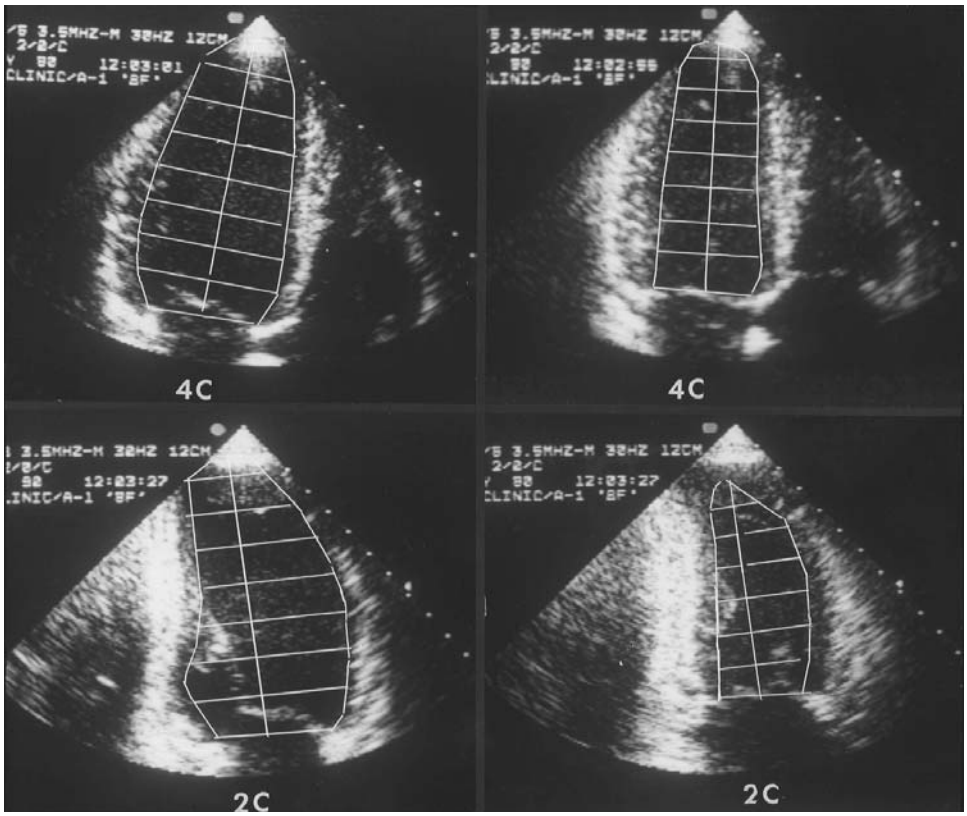

FIGURE e20-1 Still frame images of an echocardiogram in diastole (*left*) and systole (*right*). Apical four-chamber view (***top***) and apical two-chamber view (***bottom***) comprise two orthogonal views. This illustrates the quantitative assessment of ejection fraction. The endocardial area is outlined and is used for calculation of ejection fraction.

With quantitative two-dimensional echocardiography, endocardial outlines of the left ventricle (LV) cavity are traced in systole and diastole and the LV cavity areas are then fitted to computer models of the LV to obtain systolic and diastolic volumes. The presence or absence of regional wall motion abnormalities can be assessed by examining endocardial motion as well as wall thickening.

VIDEO e20-2 Real-time echocardiographic images of a patient with a severe decrease in left ventricular systolic function. The estimated ejection fraction is 20%. ***A.*** (Play video) Parasternal long axis view. ***B.*** (Play video) Parasternal short axis view.

VIDEO e20-3 Real-time echocardiographic images of a patient with hypertrophic cardiomyopathy, demonstrating an increase in wall thickness during systole. ***A.*** (Play video) Parasternal long axis view. ***B.*** (Play video) Parasternal short axis view.

VIDEO e20-4 Real-time echocardiographic images of a patient with mitral stenosis. There is diastolic doming and restricted leaflet opening secondary to fusion of the commissures. ***A.*** (Play video) Parasternal long axis. ***B.*** (Play video) Parasternal short axis.

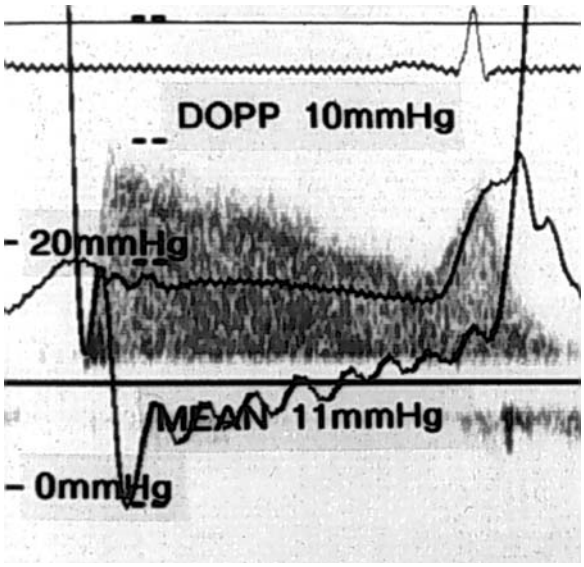

FIGURE e20-2 Continuous wave Doppler (DOPP) echocardiographic tracings across the mitral valve in a patient with mitral stenosis with simultaneous pressures in the left atrium (LA) and left ventricle (LV). The velocity of flow is high in early diastole, followed by a prolonged deceleration of transmitral mitral flow velocity, and a re-acceleration during atrial systole (A). There is a mean gradient of 10 mmHg derived from the Doppler tracing, which corresponds to the simultaneous transmitral gradient of 11 mmHg derived from cardiac catheterization. These are consistent with the diagnosis of moderate mitral stenosis. LA, left atrial pressure; LV, left ventricular pressure; a, atrial contraction wave. *(From RA Nishimura et al: J Am Coll Cardiol 24:152, 1994.)*

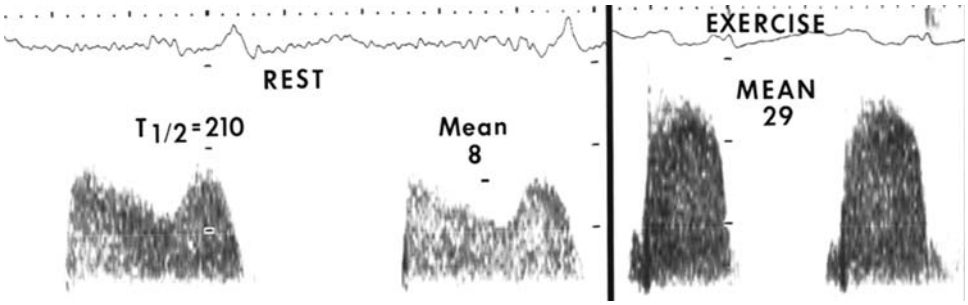

FIGURE e20-3 Continuous-wave Doppler echocardiogram across the mitral valve of a patient with mitral stenosis. In the resting state (***left***) there is a mean gradient of 8 mmHg. During exercise (***right***), the mean gradient rises to 29 mmHg, indicating hemodynamically significant mitral stenosis.

VIDEO e20-5 Real-time images with color-flow Doppler imaging of a patient with mitral regurgitation due to ruptured chordae tendinae. *A.* (Play video) Gray scale image showing a thickened redundant posterior leaflet with loss of coaptation. ***B.*** (Play video) Color-flow imaging showing the regurgitation as a high-velocity turbulence (mosaic pattern) regurgitating into the left atrium during systole. ***C.*** (Play video) Color-flow imaging of a patient with a normal mitral valve showing no regurgitation into the left atrium.

VIDEO e20-6 (Play video) **Real-time transesophageal echocardiographic images of a patient with severe mitral regurgitation** due to a flail posterior leaflet. The posterior mitral valve leaflet is completely unsupported and moves into the left atrium during systole.

VIDEO e20-7 Real-time echocardiographic images from the parasternal long axis view of a patient with mitral valve prolapse. Both leaflets prolapse into the left atrium during systole. ***A.*** (Play video) Black and white images demonstrating leaflet morphology and motion. ***B.*** (Play video) Color-flow imaging demonstrating a late systolic blue-colored jet of mitral regurgitation.

Annular dilatation, prolapse, flail leaflets, vegetation, and rheumatic involvement can all be diagnosed and the LV response to volume overload assessed by two-dimensional echocardiography.

VIDEO e20-8 (Play video) **Real-time two-dimensional echocardiographic images of a patient with a vegetation on the mitral valve.** There is a mobile echo density attached directly to the mitral valve apparatus.

VIDEO e20-9 (Play video) **Real-time two-dimensional parasternal long axis echocardiographic images from a patient with aortic stenosis.** The aortic valve is calcified with restricted opening.

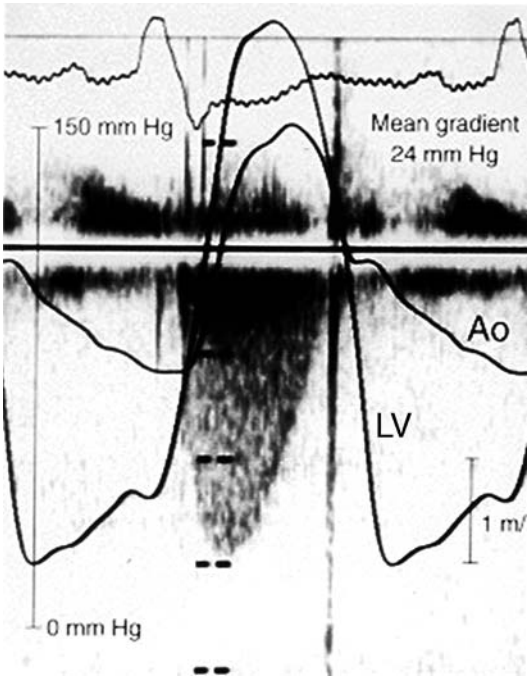

FIGURE e20-4 Continuous-wave Doppler tracings across the aortic valve in a patient with aortic stenosis. There is an increase in velocity to 3 m/s, with a mean transvalvular gradient calculated to be 24 mmHg. This corresponds to the simultaneous catheterization gradient of 24 mmHg between left ventricle (LV) and aorta (Ao).

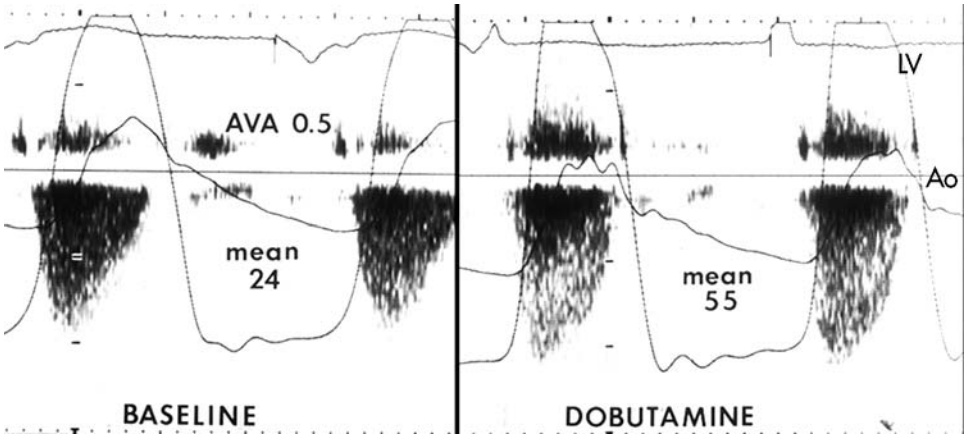

FIGURE e20-5 Continuous-wave Doppler echocardiogram across the aortic valve in a patient with low output–low gradient aortic stenosis and a reduced ejection fraction. ***Left.*** At baseline, there is a mean left ventricular (LV)-aortic (Ao) gradient of 24 mmHg (by Doppler) with a calculated aortic valve area (AVA) of 0.5 cm^2. This presents a diagnostic dilemma as the reduced aortic valve area may be due to either critical aortic stenosis and secondary LV dysfunction or a low-output state, in which there is not enough force to open fully a mildly stenotic aortic valve. ***Right.*** During dobutamine infusion, there is an increase in the transvalvular pressure gradient to 55 mmHg, with normalization of the stroke volume. This indicates the presence of severe aortic stenosis.

VIDEO e20-10 Real-time echocardiographic images showing a close-up view of the atrial septum in a patient with a large secundum atrial septal defect. *A.* (Play video) Gray scale image showing a questionable "drop-out" in the atrial septum. ***B.*** (Play video) Color-flow imaging confirms flow across the atrial septum.

VIDEO e20-11 (Play video) **Real-time transesophageal echocardiographic images of a patient with a left atrial myxoma.** There is a large echo-dense mass in the left atrium that is attached to the atrial septum. The mass moves across the mitral valve in diastole.

Although an echocardiographic examination cannot provide pathologic confirmation of the etiology of a mass, in many instances the diagnosis can be suspected from the appearance, mobility, attachments, and concomitant abnormalities.

VIDEO e20-12 (Play video) **Real-time two-dimensional echocardiographic images of a patient with a pericardial effusion.** The effusion is shown as black echo-free space surrounding the heart.

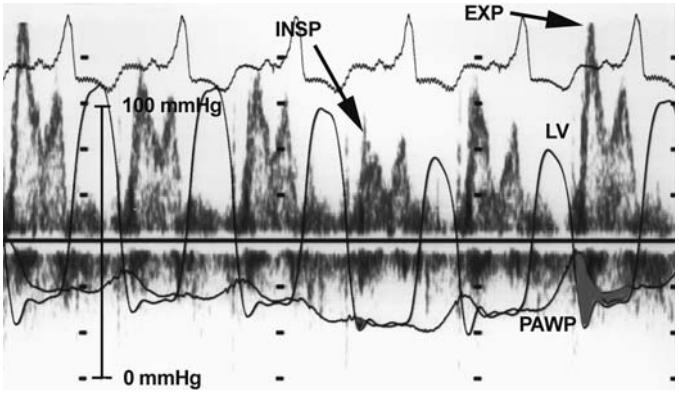

FIGURE e20-6 Pulsed-wave Doppler echocardiogram of transmitral flow recorded simultaneously with pulmonary artery wedge pressure (PAWP) and left ventricular (LV) pressure in a patient with constrictive pericarditis. There is a dissociation of intrathoracic and intracardiac pressures so that the PAWP has a larger inspiratory (INSP) fall than the LV pressure, causing a decrease in the driving force across the mitral valve. This results in a fall in the transmitral flow velocity. The opposite occurs during expiration (EXP).

VIDEO e20-13 (Play video) **Real-time two-dimensional echocardiographic images from the parasternal long axis view of a patient with a large aneurysm of the ascending aorta.**

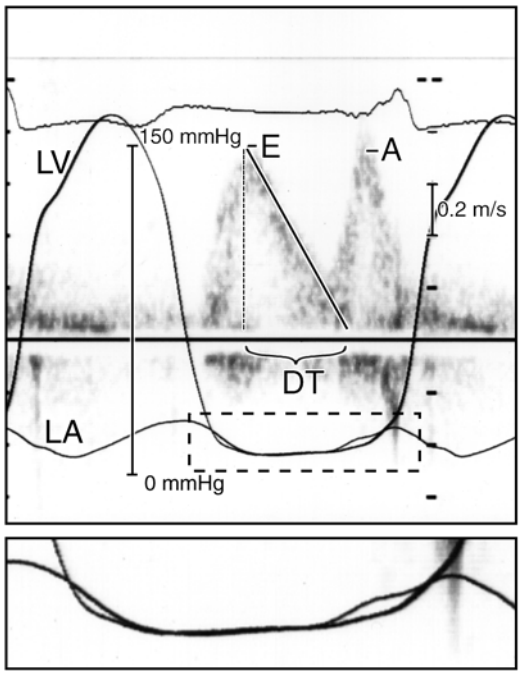

FIGURE e20-7 Pulsed-wave Doppler tracings of the mitral valve inflow velocities superimposed on left atrial (LA) and left ventricular (LV) pressures. The initial (early diastolic) velocity of mitral inflow (E) correlates with the driving pressure across the mitral valve. The deceleration time (DT) indicates the relative change in LA and LV pressures as blood begins to fill the LV. This increases LV pressure, which rises to meet the LA pressure. The A velocity on the mitral flow velocity curve is a reacceleration of flow due to atrial contraction. Normally, the E velocity exceeds the A velocity. In this patient, they are equal, suggestive of mild diastolic dysfunction (see Fig. e20-8).

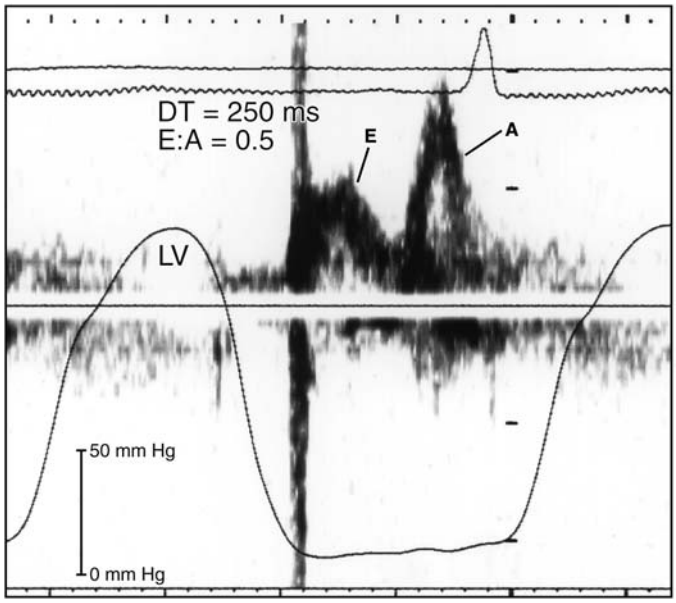

FIGURE e20-8 High-fidelity left ventricular pressure (LV) curve superimposed on a mitral inflow velocity curve obtained by Doppler echocardiography in a patient with stage I diastolic dysfunction. There is a decrease in the early diastolic filling and an increase with filling at atrial contraction, resulting in a low E:A ratio and prolonged deceleration time (DT). The LV diastolic pressure is normal at 12 mmHg.

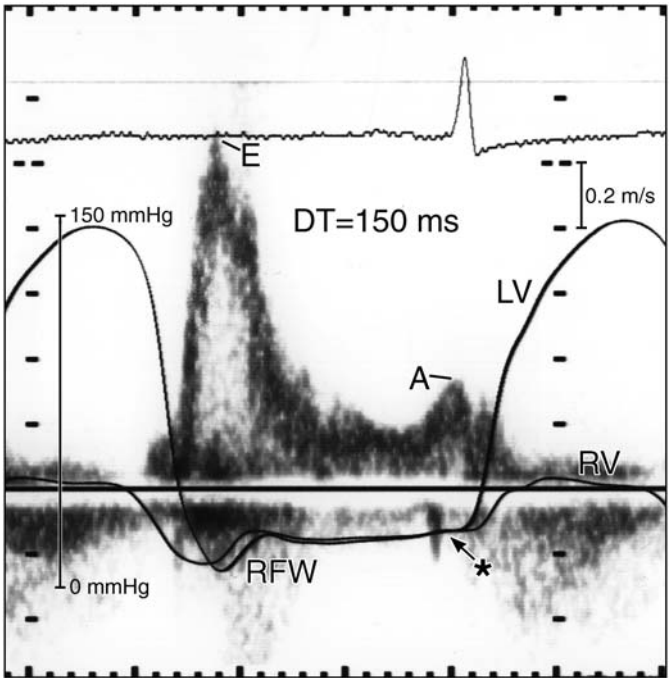

FIGURE e20-9 High-fidelity left ventricular (LV) and right ventricular (RV) pressure tracings superimposed on a Doppler mitral inflow velocity tracing in a patient with stage III diastolic dysfunction. There is a restriction to filling, in which there is a high early diastolic velocity [rapid filling wave (RFW)] and low velocity of atrial contraction resulting in a high E:A ratio with a short (150 ms) deceleration time (DT). Both ventricular diastolic pressures (*) are elevated.

VIDEO e20-14 Real-time two-dimensional stress echocardiogram in a normal subject. The studies at rest are shown on the left and the studies during peak exercise are on the right. ***A.*** (Play video) Parasternal long axis (*top*) and short axis (*bottom*) views. ***B.*** (Play video) Apical four-chamber (*top*) and two-chamber (*bottom*) views. At rest, there is contraction of all segments of the myocardium. During exercise, there are increases in contractility and in the thickening of all segments of the myocardium.

VIDEO e20-15 Real-time two-dimensional stress echocardiogram of a patient with coronary artery disease. The studies at rest are shown on the left and the studies during peak exercise are on the right. ***A.*** (Play video) Parasternal long axis (*top*) and short axis (*bottom*) views. ***B.*** (Play video) Apical four-chamber (*top*) and two-chamber views (*bottom*). The images during peak exercise show regional wall motion abnormalities in the anteroapical distribution indicative of myocardial ischemia.

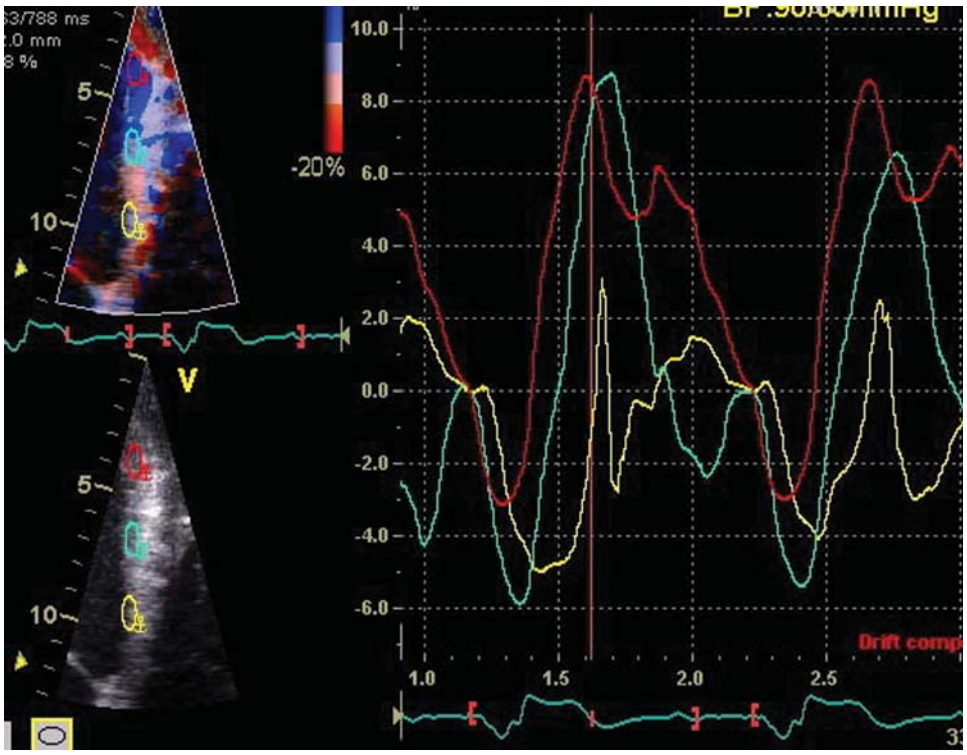

FIGURE e20-10 Strain rate images from a patient with severe left ventricular dysfunction illustrating dyssynchronous contraction.

Strain rate is a measure of regional deformation (or contraction). Strain rates can be used to examine the degree of dyssynchronous contraction of the ventricle, which may help in determining patients who would benefit from biventricular pacing. Shown are the different strain rates over time of the basal septum (yellow line), mid septum (blue line), and apical septum (red line).

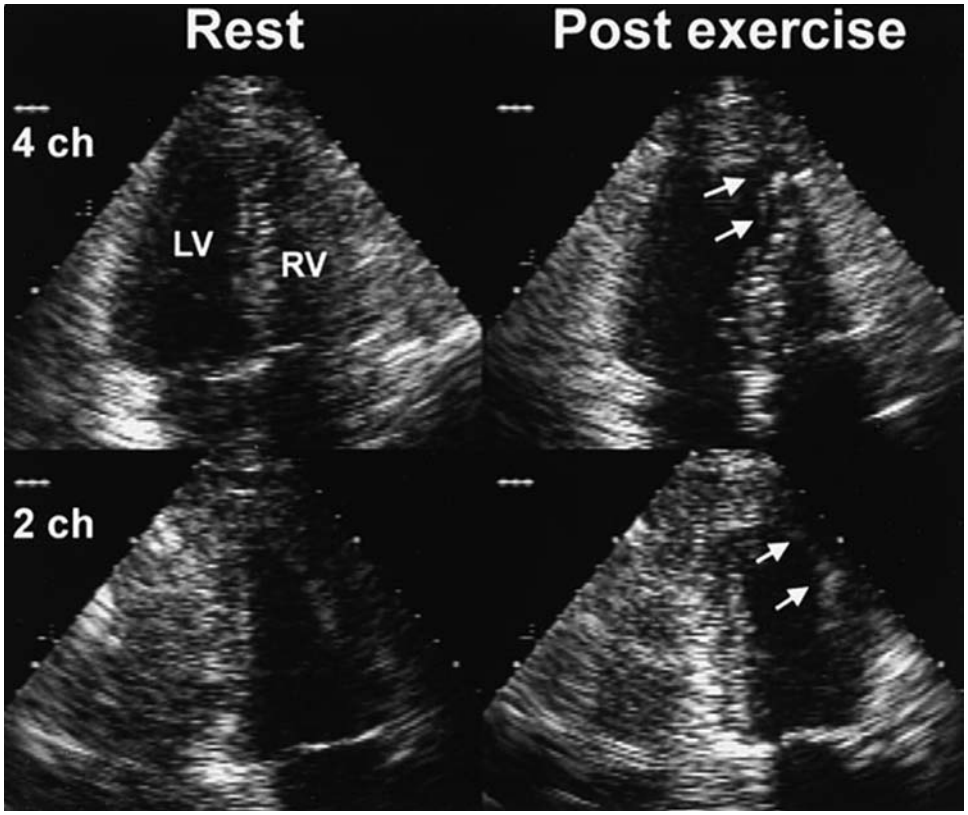

FIGURE e20-11 Still frame images demonstrating regional wall motion abnormalities during an exercise echocardiogram in a patient with known coronary artery disease. ***Left.*** The systolic frames in the resting state show symmetric contraction of all segments of the myocardium. The upper frame is from the apical four-chamber view and the lower frame is from the apical two-chamber view. ***Right.*** The systolic frames immediately after exercise show regional wall motion abnormalities in the anterior and apical segments (*arrows*). LV, left ventricle; RV, right ventricle *(From JK Oh et al: The Echo Manual, 2d ed. Philadelphia, Lippincott Williams & Wilkins, 1999, with permission.)*

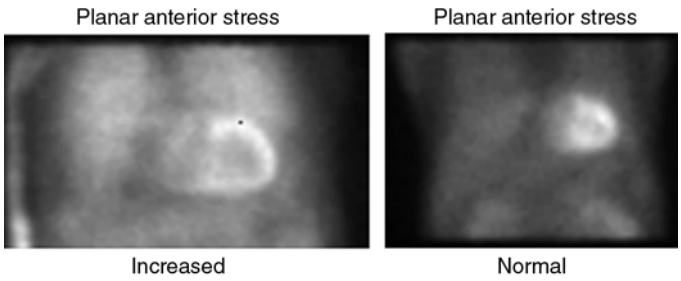

FIGURE e20-12 Anterior planar thallium images following stress, showing increased lung uptake on the left (count intensity in lung >50% of that in myocardium) and normal lung uptake on the right (count intensity in lung <50% of that in myocardium).

Increased lung uptake of thallium may be seen immediately after stress. It reflects increased pulmonary capillary wedge pressure and occurs in the presence of severe coronary artery disease and/or left ventricular dysfunction. It provides important adverse prognostic information that is incremental to other clinical, stress, and coronary angiographic variables.

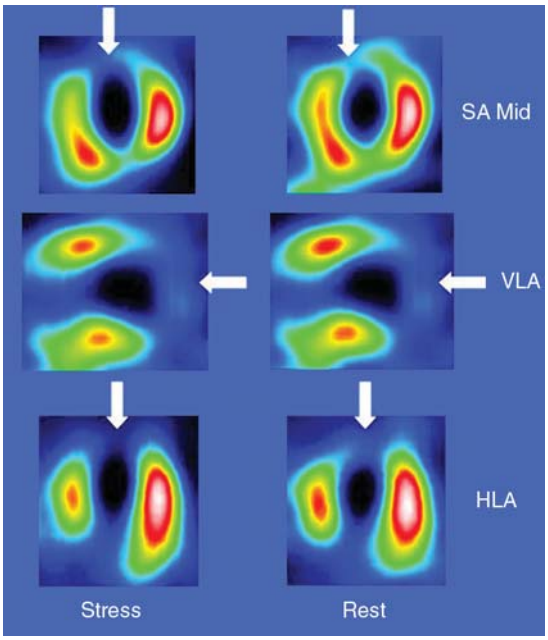

FIGURE e20-13 Adenosine ^{99m}Tc sestamibi scan in a 50-year-old male with a previous anterior infarct. The stress images (***left***) show a large defect involving the apex and anterior walls (*white arrows*) with little change from the rest images (*white arrows*), signifying a fixed defect without further ischemia during stress. SA, short axis in the middle of the left ventricle; VLA, vertical long axis; HLA, horizontal long axis.

The relative advantage of ^{201}Tl and ^{99m}Tc are detailed in **Table e20-1**. The better image quality and assessment of ventricular function permitted by ^{99m}Tc compounds have contributed to their more common use for stress imaging, although both ^{201}Tl- and ^{99m}Tc-labeled compounds provide clinically useful myocardial perfusion images in the majority of patients. A "dual-isotope" protocol is employed in some centers. This uses ^{201}Tl for the initial rest image and a ^{99m}Tc-labeled compound for the subsequent stress image, primarily for patient and scheduling convenience.

TABLE e20-1 RELATIVE ADVANTAGES OF THALLIUM 201 AND TECHNETIUM 99M

Thallium
Lower radiopharmaceutical cost
Measurement of increased pulmonary uptake
Less hepatobiliary and bowel uptake
Detection of resting ischemia (hibernating myocardium)
Technetium
Better image quality (particularly in obese patients)
Ventricular function assessment (gated SPECT)
Shorter imaging time
Shorter imaging protocols (patient/scheduling convenience)
Acute imaging in myocardial infarction and unstable angina
Superior quantification

SPECT, single photon emission computed tomography.

VIDEO e20-16 (Play video) MRI scan in real-time of a patient with a large left ventricular apical aneurysm. The long axis view demonstrates a thin dyskinetic apical aneurysm with preserved systolic function of the basal anterior and basal inferior wall.

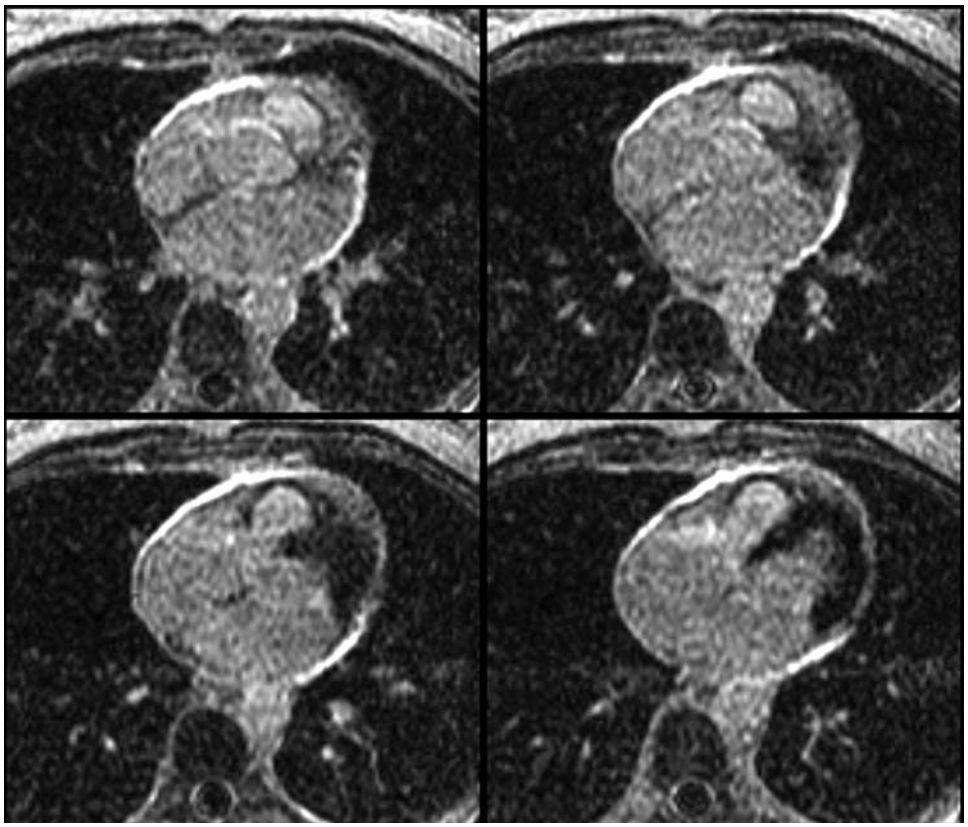

FIGURE e20-14 MR images with contrast enhancement of a patient with constrictive pericarditis, demonstrating abnormal pericardial thickening.

VIDEO e20-17 (Play video) **Three-dimensional reconstruction of an MR angiogram,** showing a severe coarctation of the descending aorta. The large collateral vessels as a result of the coarctation are shown.

VIDEO e20-18 (Play video) **Cine MR scan of a patient with a dilated ascending aorta** (annulo-aortic ectasia). There is a thin central jet of aortic regurgitation going into the left ventricular outflow tract.

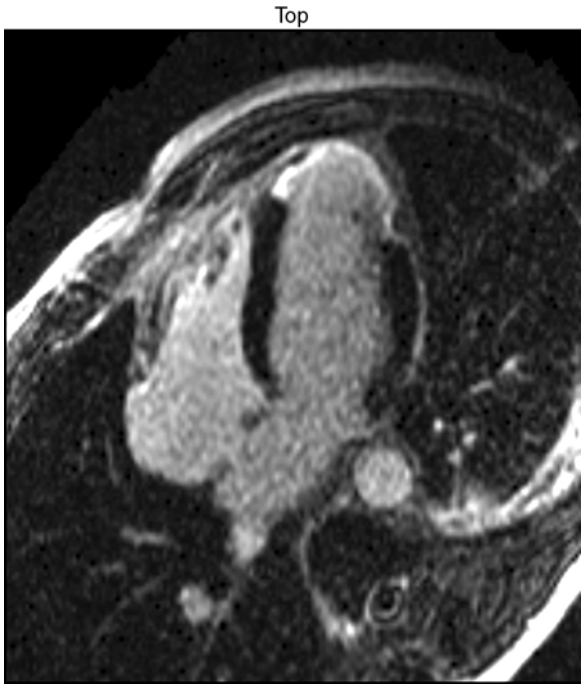

FIGURE e20-15 MR scan with delayed enhancement of a patient with an apical left ventricular infarction (*top*). Imaging the heart 10–20 min after gadolinium injection demonstrates enhancement of the infarcted tissue (visible as dense white image), as the tissue retains contrast by virtue of its large extracellular volume.

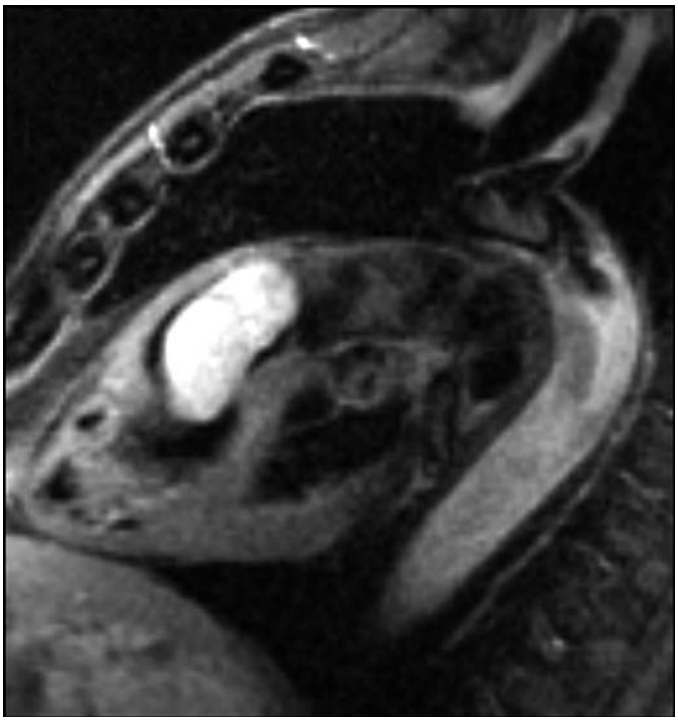

FIGURE e20-16 MR image of a patient with a right ventricular myxoma, which is shown as a bright oblong structure in the right ventricular outflow tract.

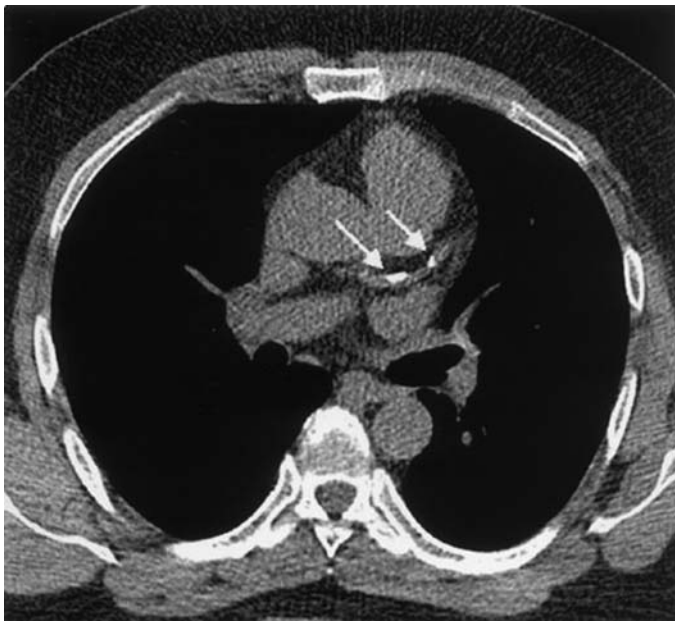

FIGURE e20-17 Noncontrast image from electron beam CT revealing two small foci of calcification in the left anterior descending artery (*arrows*).

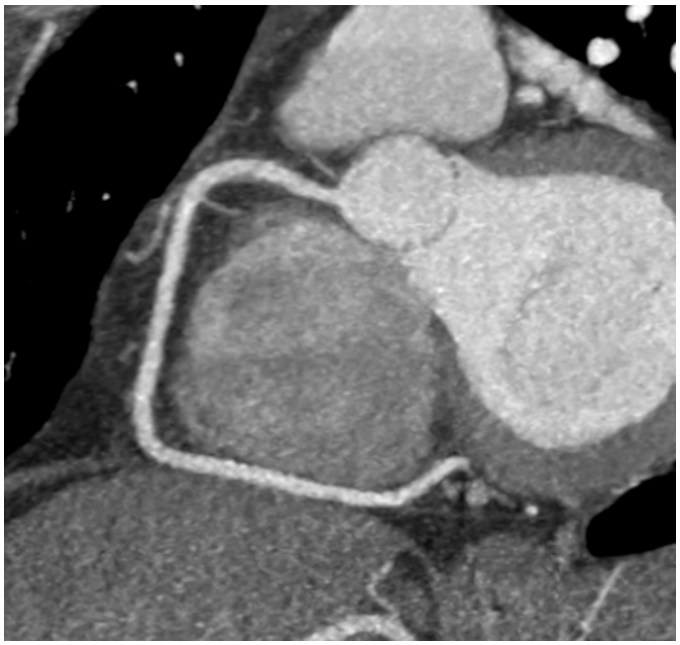

FIGURE e20-18 CT coronary angiogram showing a normal right coronary artery.

VIDEO e20-19 (Play video) CT coronary angiogram showing a normal right coronary artery. The movie highlights multiple thin slices through the right coronary artery.

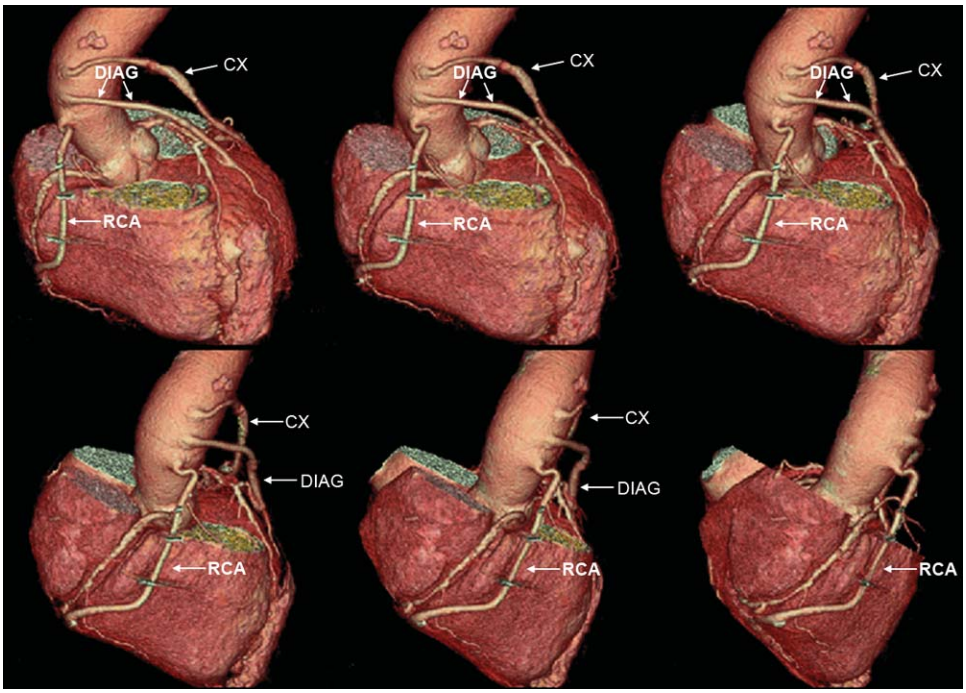

FIGURE e20-19 Three-dimensional reconstruction of a CT angiogram demonstrating three saphenous vein coronary artery bypass grafts in different views. In the upper left panel is an anterior-posterior view of the heart and grafts. The heart is sequentially rotated clockwise in the panels going from left to right to illustrate the ability of CT angiography to visualize the saphenous vein grafts. RCA, saphenous vein graft to the right coronary artery; CX, saphenous vein graft to the circumflex artery; DIAG, saphenous vein graft to the diagonal artery.

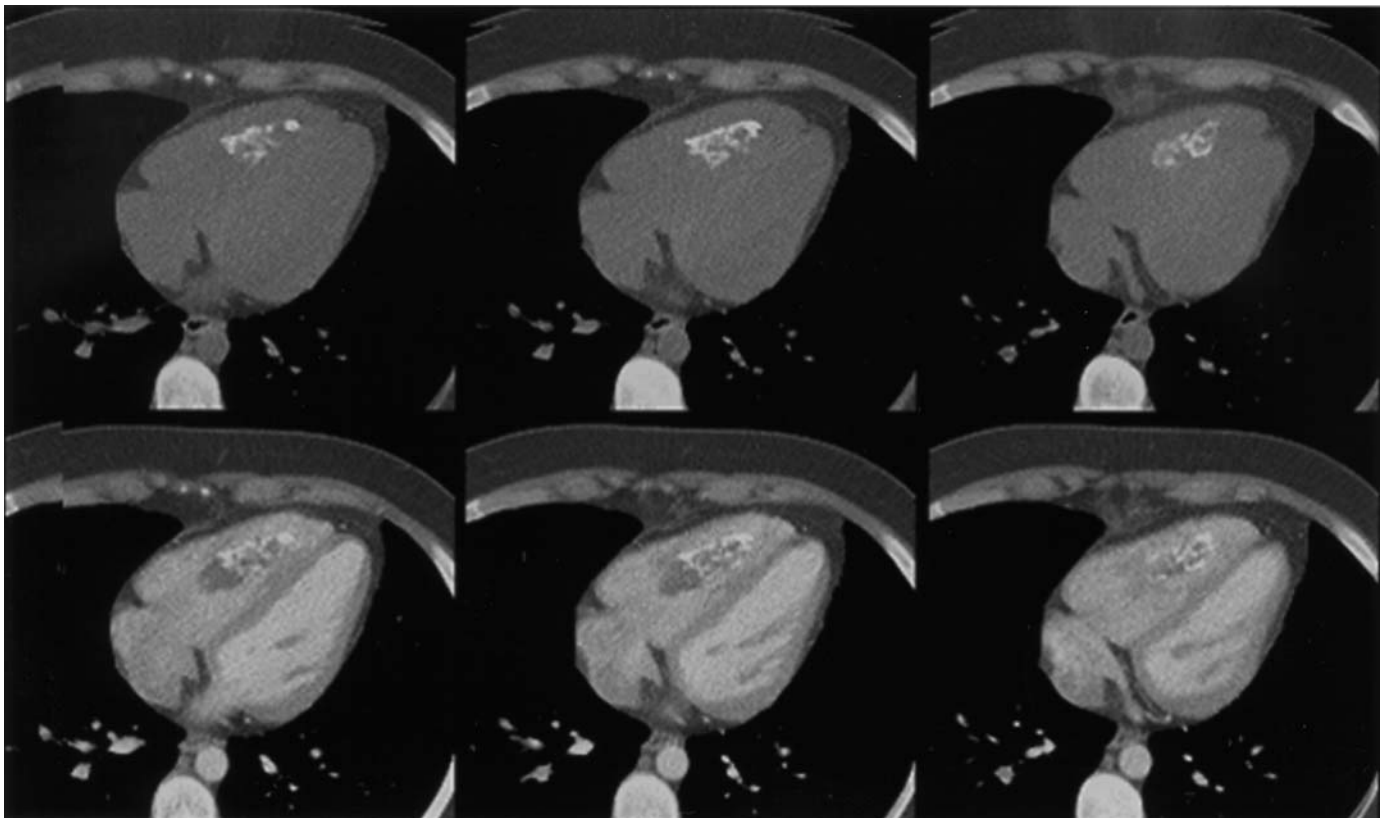

FIGURE e20-20 Cardiac CT images demonstrating a calcified mass in the right ventricle, which at pathologic examination was a chronic thrombus. Calcification is seen as a bright signal in both the noncontrast (*upper*) and contrast-enhanced (*lower*) images.